agriculture

MDPI

Article

Toxicity of Ethyl Formate to *Tribolium castaneum* (Herbst) Exhibiting Different Levels of Phosphine Resistance and Its Influence on Metabolite Profiles

Changyao Shan [1,2,3], Xinyue You [1,4], Li Li [1], Xin Du [2], Yonglin Ren [2,3,*] and Tao Liu [1,4,*]

[1] Institute of Equipment Technology, Chinese Academy of Inspection and Quarantine, No. A3, Gaobeidianbeilu, Chaoyang District, Beijing 100123, China; 34424808@student.murdoch.edu.au (C.S.); sy20223193241@cau.edu.cn (X.Y.); lili@caiq.org.cn (L.L.)
[2] Harry Butler Institute, Murdoch University, Murdoch, WA 6150, Australia; b.du@murdoch.edu.au
[3] College of Environmental and Life Sciences, Murdoch University, Murdoch, WA 6150, Australia
[4] Department of Plant Biosecurity, College of Plant Protection, China Agricultural University, Beijing 100193, China
* Correspondence: y.ren@murdoch.edu.au (Y.R.); liut@caiq.org.cn (T.L.); Tel.: +61-08-409758976 (Y.R.); +86-10-85773355 (T.L.)

Abstract: Ethyl formate (EF), a naturally occurring fumigant, has attracted widespread attention owing to its low toxicity in mammals. Here, Direct Immersion Solid-Phase Microextraction (DI-SPME) was employed for sample preparation in mass spectrometry-based untargeted metabolomics to evaluate the effects on *Tribolium castaneum* (Herbst) strains with different levels of PH_3 resistance (sensitive, TC-S; moderately resistant, TC-M; strongly resistant, TC-SR) when exposed to a sublethal concentration (LC_{30}) of EF. The bioassay indicated that *T. castaneum* strains with varying PH_3 resistance levels did not confer cross-resistance to EF. A metabolomic analysis revealed that exposure to sublethal doses of EF significantly altered 23 metabolites in *T. castaneum*, including 2 that are unique to the species which remained unaffected by external conditions, while 11 compounds showed a strong response. A pathway topology analysis indicated that EF caused changes to several metabolic pathways, mainly involving fatty acids and their related metabolic pathways. This study showed that EF can induce highly similar metabolic responses in insects across varying levels of PH_3 resistance, suggesting that the mechanisms driving the toxicity of EF and PH_3 are distinct. These insights significantly extend our knowledge of the toxic mechanisms of EF and provide direct evidence for the efficacy of EF treatment for managing PH_3 resistance in insects.

Keywords: *Tribolium castaneum* (Herbst); metabolites; PH_3 resistance; ethyl formate; DI-SPME-GC/MS

Citation: Shan, C.; You, X.; Li, L.; Du, X.; Ren, Y.; Liu, T. Toxicity of Ethyl Formate to *Tribolium castaneum* (Herbst) Exhibiting Different Levels of Phosphine Resistance and Its Influence on Metabolite Profiles. *Agriculture* **2024**, *14*, 323. https://doi.org/10.3390/agriculture14020323

Academic Editor: Anna Andolfi

Received: 26 December 2023
Revised: 13 February 2024
Accepted: 16 February 2024
Published: 18 February 2024

1. Introduction

Phosphine (PH_3) and methyl bromide (MB) are currently the two most widely used fumigants. MB is a broad-spectrum fumigant that controls insects, nematodes, fungi, and bacteria [1,2]. It has been extensively employed for grain fumigation, soil disinfection, quarantine, and the sterilization of transportation equipment. However, MB causes significant damage to the ozone layers. The Montreal Protocol stipulated that developed countries completely phased out the use of MB in 2005, while developing countries followed suit in 2015 [3]. Therefore, PH_3 is currently the only widely accepted fumigant. PH_3 has strong penetration, leaves a low level of residue after fumigation, and has extensive applications in grain storage [4]. Fumigation with phosphine requires a long exposure time; the long-term and unreasonable use of PH_3 has led to the development of PH_3 resistance in numerous pests worldwide [5]. PH_3 resistance in stored grain pests poses a significant threat to international trade, especially in countries like Australia that insist on a "zero-tolerance" policy for exported produce [5,6].

Ethyl formate (EF) is a fumigant that has been studied as a potential alternative to PH_3 for pest control in stored grains and food commodities [7]. EF has fast action, high efficacy, low residue, and low environmental toxicity. Studies have demonstrated that EF has comparable or even superior fumigation efficacy to PH_3 for the control of a range of pests associated with stored grain, including *Sitophilus oryzae*, *T. castaneum*, and *Rhyzopertha dominica* [8]. Ren et al. found that EF had significantly higher mortality rates for *S. oryzae* and *T. castaneum* compared to PH_3, while the residues of EF fall below the Australian maximum residue level (MRL) of 1.0 mg/kg in dried fruit) [9]. Others found that fumigation was effective in controlling both PH_3-resistant and susceptible strains of *Liposcelis bostrychophila* and *S. oryzae* [10,11]. These findings suggest that EF has great potential as a fumigant for pest control in stored grains.

The toxicological mechanisms of EF fumigation in insects have been studied from proteomic and enzymological perspectives. Exposure to EF inhibited mitochondrial cytochrome C oxidase, thereby affecting insect respiration [12]. Kim et al. reported that EF inhibited acetylcholinesterase (AChE) and carboxylesterase (CarE) activities [13]. These findings suggest that the toxicological mechanisms of EF are similar to those of PH_3 [14].

Variations in metabolite levels within insects can serve as indicators of changes in the external environment. The effects of EF on insect metabolic pathways are poorly studied. Alnajim et al. reported that Direct Immersion Solid-Phase Microextraction (DI-SPME) coupled with Gas Chromatography–Mass Spectrometry (GC-MS) provides a robust, reliable, and sensitive non-derivatization extraction method for insect metabolomic research [15,16]. This study focused on the phosphine-resistant strains of *T. castaneum* adults by employing the DI-SPME technique coupled with GC-MS to investigate the changes in the metabolites of *T. castaneum* before and after EF fumigation.

In the present study, we aimed to evaluate the efficacy of EF against different PH_3-resistant strains of adult *T. castaneum*, with particular emphasis on cross-resistance to EF among the PH_3-resistant strains. Using DI-SPME coupled with GC-MS, we obtained metabolic profiles of *T. castaneum* before and after EF fumigation to better understand the toxicity mechanism of EF in *T. castaneum*.

2. Materials and Methods

2.1. Insect Culture

Cultures of PH_3-susceptible and -resistant adults of *T. castaneum* (TC-S, TC-M, and TC-SR) were provided by the Chinese Academy of Inspection and Quarantine (CAIQ). To rear narrow-aged insects, 1000 adult insects were incubated with 300 g of mixed feed consisting of wheat flour and *Saccharomyces cerevisiae* (baker's yeast) in a 9:1 ratio in a glass jar (12 cm inner diameter and 25 cm length) sealed with gauze. The wheat flour used was of domestic quality and was purchased from a food market. Before use, the flour was treated for existing storage insects by freezing at −20 °C for 7 d, followed by storage at 4 °C until use. After three days of incubation, adult insects were removed, and the remaining medium containing eggs was incubated at 25 ± 2 °C with 65 ± 5% relative humidity (RH). When adults emerged, they were transferred to a new jar with food (as above) to ensure that the uniform-aged insects remained together. The insects used in the experiments were approximately one month old.

2.2. Fumigation System

The fumigation chambers used were 6 L desiccators sealed with modified rubber plugs and Swagelok snap fittings (304 3/8 inches and 8 mm thickness, Shanghai Yihao Co., Shanghai, China). The procedure for the fumigation bioassays of PH_3 and EF was as follows:

PH_3: Ammonia-free PH_3 gas was produced by reacting aluminum phosphide tablets (Nippon Kasei Co., Ltd., Tokyo, Japan) with a 5% (*v*/*v*) sulfuric acid solution. The PH_3 concentration in the gas mixture was measured using molybdenum blue colorimetry (GB/T16037, 1996) [17]. The concentrated PH_3 gas was then transferred into a 1 L gas-tight

bag (CEL Scientific Co., Cerritos, CA, USA) equipped with an adjustable valve and a silicon diaphragm. An airtight syringe was used to extract the gas into a 6 L desiccator. For PH_3 fumigation, six different concentrations were selected for testing within the range of 0.2 to 10 mg/L over a 20 h exposure period [18].

EF: A filter paper was inserted into the rubber plug to provide an evaporation substrate for the injected liquid EF (reagent grade, 97%, Sigma-Aldrich, St. Louis, MO, USA). At the bottom of the desiccator, a small fan was placed to stir the fumigant and ensure even distribution. To assess the dose response to EF fumigation, ten concentrations ranging from 10 to 30 mg/L were tested over a 4 h exposure period [19].

Fumigation bioassays of EF and PH_3 were conducted with *T. castaneum* adults in the fumigation chambers at 25 ± 2 °C and 60 ± 5% RH. Plastic jars (40 mm i.d. × 60 mm height) were used as test insect containers. Each fumigation chamber was loaded with three jars, each containing 30 adult insects. After the fumigation process, the desiccators were aerated for 2 h. Subsequently, the treated insects were transferred to an incubator set at 25 °C and 60% RH. Mortality was assessed at 72 h post-fumigation.

2.3. Gas Measurement

Calibration and detection for EF and PH_3 were carried out based on previously established methods [19]. The concentration of EF was assessed utilizing a gas chromatograph (GC6890, Agilent Technology Co., Ltd., Santa Clara, CA, USA) equipped with a flame ionization detector (GC-FID) after separation in an HP-Innowax capillary column (30 m length × 0.25 mm i.d., film thickness of 0.25 μm; Agilent Technology Co., Ltd., Santa Clara, CA, USA). Nitrogen (99.99%) was used as the carrier gas at a flow rate of 1.2 mL/min. The oven temperature was programmed to 100 °C for 2.5 min; the injection port temperature was set at 200 °C; and the detector temperature was maintained at 250 °C [19,20]. PH_3 concentrations were tested using a gas chromatograph and thermal conductivity detector (GC-TCD) following separation with a stainless steel column (3 m length × 3 mm i.d.) packed with 80/100 mesh Porapak Q (Beijing Mingnike Analytical Instrument Equipment Center, Beijing, China). The oven temperature was set at 70 °C for 4.5 min with a carrier gas flow (H_2) of 1.8 mL/min. Both the detector and injector temperatures were set at 200 °C. After fumigation, the bottles were opened and ventilated for 2 h in a fume hood [18]. During fumigation, the concentrations of the two fumigants inside the fumigation bottles were measured at 1 h, 3 h, 6 h, and 20 h.

2.4. Solid-Phase Microextraction (SPME) Procedure and Sampling Setup

Twenty *T. castaneum* adults that remained active despite being fumigated with a sublethal concentration (LC_{30}) of EF were selected and placed in 2 mL microtubes (Eppendorf, Hamburg, Germany). The microtubes were immediately frozen with liquid nitrogen and stored in an ultra-low-temperature freezer (MDF-U73V, Sanyo Electric Co., Ltd., Osaka, Japan) at −80 °C. These samples were used to investigate the effects of EF on the metabolites of different PH_3-resistant *T. castaneum* strains [15]. Then, the insects were ground to a powder and suspended immediately in 1.5 mL of HPLC-grade acetonitrile (≥99.9%, Xilong Chemical Co., Ltd., Shantou, China). After shaking (IKA MS 3 basic, IKA, Staufen, Germany) the microtubes for 3 min at 1000 rpm, the microtubes were then centrifuged (5417R, Eppendorf, Germany) for 3 min at 25 °C and 4000 rpm. The resulting supernatant (1.3 mL) was transferred to an amber chromatography vial with a PTFE-coated septum (Supelco, Darmstadt, Germany) [21]. Untreated *T. castaneum* samples (Con-S, Con-M, and Con-SR) were maintained under fumigation conditions for 4 h as the control group, with the subjects undergoing the same procedure.

For the DI-SPME procedure, an SPME fiber (50/30 μm DVB/CAR/PDMS, Stableflex 2 cm, 57348-U, Supelco, Bellefonte, PA, USA) was used. This fiber was promptly inserted into amber chromatography vials and immersed into the sample solution for 1 h at room temperature (25 ± 1 °C). Subsequently, the fiber was taken out and directly injected into the GC-MS injector with desorption for 15 min at an inlet temperature of 270 °C to analyze

the sample. Each of the six samples (Con-S, Con-M, Con-SR, EF-S, EF-M, and EF-SR) was analyzed in triplicate [15].

2.5. Gas Chromatography–Mass Spectrometry (GC-MS) Conditions

An Agilent 8890 gas chromatograph (GC) was used with an HP-5MS capillary column (30 m × 0.25 mm, 0.25 µm; Agilent J&W Scientific, Santa Clara, CA, USA) and an Agilent 5977B mass selective detector (MSD). The carrier gas used was 99.999% purified helium at a constant flow rate of 1 mL/min. The GC conditions used were as follows: injection temperature of 270 °C and an initial oven temperature of 60 °C for 2 min, which was then increased to 200 °C at the rate of 7 °C/min, and then increased to 300 °C at the rate of 5 °C/min, and finally increased to 320 °C at a rate of 50 °C/min and maintained for 3 min. The MS parameters were as follows: the transmission line temperature of the ion source was 230 °C, the transfer line temperature of the MSD was 280 °C, and the quadrupole temperature was 150 °C. Information was collected using the full scanning mode of the mass spectrometer; the mass scanning range was 30 to 500 atomic mass units (amu), and the solvent delay time was 4.5 min. The total running time was 45.4 min [15].

2.6. Statistical Analysis

The GC-MS data were preliminarily identified using Agilent MasterHunter Qualitative Analysis 10.0 and recorded and sorted using Microsoft Excel. Most metabolites were further identified using the National Institute of Standards and Technology (NIST) and the Wiley Registry of Mass Spectral Data as well as the retention index provided by the compound database of the NIST Chemistry Web Book [22].

The XCMS package in RStudio (Version: 2021.9.0) was used to extract and analyze the feature data of the GC-MS data. The edited data matrix was imported into RStudio and a Principal Component Analysis (PCA), Orthogonal Partial Least Squares Discriminant Analysis (OPLS-DA), Hierarchical Cluster Analysis (HCA), and Artificial Neural Network (ANN) analysis were performed using R (version 4.3.0) and MATLAB (version 2022b). Differential metabolites were screened according to the Variable Importance in the Projection (VIP) value and Student's *t*-test, and significant differences among the experimental groups were analyzed. The pathways of the differential metabolites were further screened using enrichment analysis to identify the key pathways with the highest correlation with the differential metabolites.

3. Results

3.1. Phosphine Susceptibility Tests

The probit analysis of adult mortality of three strains of *T. castaneum* adults (Wuhan, Qihe, and Shenzhen) indicated that the responses to PH_3 concentrations fit well with the complementary log–log and probit–log regression models, respectively, in each species, with a significant ($p < 0.001$) mean deviance ratio. The three tested strains of *T. castaneum* exhibited high variability (heterogeneity > 1), indicating that the observed mortality response to PH_3 was dispersed [6]. The index of significance of the potency estimation G-factor for the mortality response data of adults of all three strains was below the threshold index of 0.5 and in the range of 0.119–0.331. Consequently, based on the estimated G-factor values, the predicted confidence intervals for lethal concentrations at different probability levels remained accurate, even if the mortality response data were highly heterogeneous.

The resistance ratio is typically calculated at a 50% mortality rate using the FAO method. The LC_{50} of the susceptible strain exposed for 20 h was 0.0088 mg/L (95% fiducial limits: 0.0085–0.0090 mg/L) [23]. The adults of *T. castaneum* resistant to PH_3 were classified into different levels: susceptible, low resistance (1 < RR < 10), moderate resistance (10 < RR < 100), and strong resistance (RR > 100) [24,25]. In this study, the Wuhan, Qihe, and Shenzhen strains exhibited susceptibility (TC-S), moderate resistance (TC-M), and strong resistance (TC-SR) (Table 1).

Table 1. Probit mortality response of adults of *Tribolium castaneum* (Herbst) to phosphine at 25 ± 2 °C and 55 ± 5% RH.

Strain (Response Phenotype [a])	N [b]	Slope ± SE	LC_{30} (mg/L) (95%FL [c])	LC_{50} (mg/L) (95%FL)	LC_{99} (mg/L) (95%FL)	Heterogeneity Factor	*df* [d]	G-Factor [e]	Mean Deviance Ratio [f]	RR [g] (CL [h])	Classification
TC-S (Con-S)	450	1.667 ± 0.242	0.004 (0.000, 0.010)	0.009 (0.003, 0.014)	0.223 (0.080, 1.089)	1.858	16	0.331	63.262 ($p < 0.001$)	-	Susceptibility
TC-M (Con-M)	540	1.880 ± 0.176	0.122 (0.084, 0.157)	0.232 (0.184, 0.285)	4.010 (2.211, 10.993)	1.060	16	0.140	80.178 ($p < 0.001$)	25.778 (18.120, 33.991)	Moderate
TC-SR (Con-SR)	540	3.359 ± 0.290	5.323 (4.012, 6.372)	7.626 (6.371, 9.064)	37.579 (24.559, 87.334)	2.040	16	0.119	54.434 ($p < 0.001$)	847.333 (645.920, 1069.069)	Strong

[a] Response phenotype: TC-S, susceptible; TC-M, moderate resistance; TC-SR, strong resistance. [b] N: Total number of insects used for the bioassay. [c] FL: Fiducial limit. [d] *df*: Degrees of freedom. [e] G-factor = $[t^2 \times V(b)/b^2]$, where t is Student's t with error degrees of freedom, $V(b)$ is the slope variance estimate given in the variance–covariance matrix, and b is the slope estimate. G-values that are less than 0.5 suggest that the value of the mean is within the limit at 95% probability. [f] Fisher's probability value is highly significant (<0.001). [g] Resistance ratio (RR): LC_{50} of resistant strain/LC_{50} of susceptible strain. [h] CL: Confidence interval.

3.2. Susceptibility and Test for Cross-Resistance to EF

An analysis of the dose–mortality response of *T. castaneum* adults to EF produced highly significant deviance ratios ($p < 0.001$) with low heterogeneity values (heterogeneity < 1). The g-factor values were well below the reference index of 0.5 and remained in the range of 0.034–0.040 for the adult data of the three strains. This suggests that the adults responded strongly to EF over a series of concentrations and that the confidence intervals of the lethal estimates were valid [6].

The dose–mortality response to EF in phosphine-susceptible (TC-S) and phosphine-resistant (TC-M and TC-SR) strains demonstrated the absence of cross-resistance to EF in the phosphine-resistant strains. The overlapping fiducial limits among the LC_{30}, LC_{50}, and LC_{99} values and the insignificant confidence intervals, which were estimated based on the resistance ratio of *T. castaneum*, indicated that the intervals carrying less than 1.0, between the PH_3-susceptible and -resistant strains, confirmed the absence of significant differences in these strains in their responses to EF (Table 2) [6,26].

Table 2. Probit mortality response of adults of phosphine-susceptible (TC-S) and -resistant (TC-M and TC-SR) strains of *Tribolium castaneum* (Herbst) to ethyl formate at 25 ± 2 °C and 65 ± 5% RH.

Strain (Response Phenotype [a])	N [b]	Slope ± SE	LC_{30} (95%FL [c])	LC_{50} (95%FL)	LC_{99} (95%FL)	Heterogeneity Factor	*df* [d]	G-Factor [e]	Mean Deviance Ratio [f]	RR [g] (CL [h])
TC-S (EF-S)	900	15.138 ± 0.980	16.833 (16.407, 17.218)	18.230 (17.850, 18.610)	25.970 (24.877, 27.415)	0.916	16	0.038	158.212 ($p < 0.001$)	-
TC-M (EF-M)	900	14.995 ± 0.996	16.006 (15.584, 16.384)	17.348 (16.974, 17.719)	24.797 (23.732, 26.216)	0.460	16	0.040	110.284 ($p < 0.001$)	0.952 (0.872, 1.033)
TC-SR (EF-SR)	900	11.918 ± 0.736	14.497 (14.042, 14.906)	16.043 (15.636, 16.443)	25.146 (23.906, 26.780)	0.498	16	0.034	90.786 ($p < 0.001$)	0.880 (0.806, 0.955)

[a] Response phenotype: TC-S, susceptible; TC-M, moderate resistance; TC-SR, strong resistance. [b] N: Total number of insects used for the bioassay. [c] FL: Fiducial limit. [d] *df*: Degrees of freedom. [e] G-factor = $[t^2 \times V(b)/b^2]$, where t is Student's t with error degrees of freedom, $V(b)$ is the slope variance estimate given in the variance–covariance matrix, and b is the slope estimate. G-values that are less than 0.5 suggest that the value of the mean is within the limit at 95% probability. [f] Fisher's probability value is highly significant (<0.001). [g] Resistance ratio (RR): LC_{50} of resistant strain/LC_{50} of susceptible strain. [h] CL: Confidence interval.

3.3. Metabolite Expression in Response to EF in Different Levels of PH_3 Resistance

In *T. castaneum*, a GC-MS analysis revealed significant differences in the responses of 23 of the 25 detected compounds between the control and EF treatment groups (Figure 1). Compound identification between the control and treatment groups revealed that 15 compounds were significantly upregulated after the EF treatment, with 1-(2-Hydroxy-4-methoxyphenyl)

propane-1-one showing the lowest *p*-value ($p = 1.87 \times 10^{-8}$) and the highest statistical difference in relative abundance between the two groups. Eight compounds showed significantly lower levels than in the control group. These compounds were orcinol, 2-undecenal, pentacosane, 11-methylheptacosane, hexacosane, 13-methylheptacosane, octacosane, and 15-methylnonacosane; 15-methylnonacosane was the most significantly downregulated. An analysis also indicated that 1-pentadecene and triacontane were not statistically different in relative abundance between the EF-treated group and the control group, with a *p*-value higher than the confidence interval ($p \geq 0.05$). This finding is consistent with previous research, where 1-pentadecene was reported as an odoriferous gland product in *T. confusum* [27,28], and triacontane was reported as the main constituent of the cuticle layer of *T. castaneum* [15]. Furthermore, within the identified compounds, we observed that the relative abundance variations in 1-hexadecanol, hexacosane, octacosane, and lathosterol were solely influenced by the EF treatment and were unrelated to the PH_3 resistance level of *T. castaneum*, whereas the variations in 2-methyl-p-Benzoquinone and 2-ethyl-p-Benzoquinone appeared to be influenced not only by the EF treatment but also by the level of resistance to PH_3. This suggests that these benzoquinone derivatives have the potential to serve as biomarkers for identifying PH_3 resistance in *T. castaneum* (Table 3).

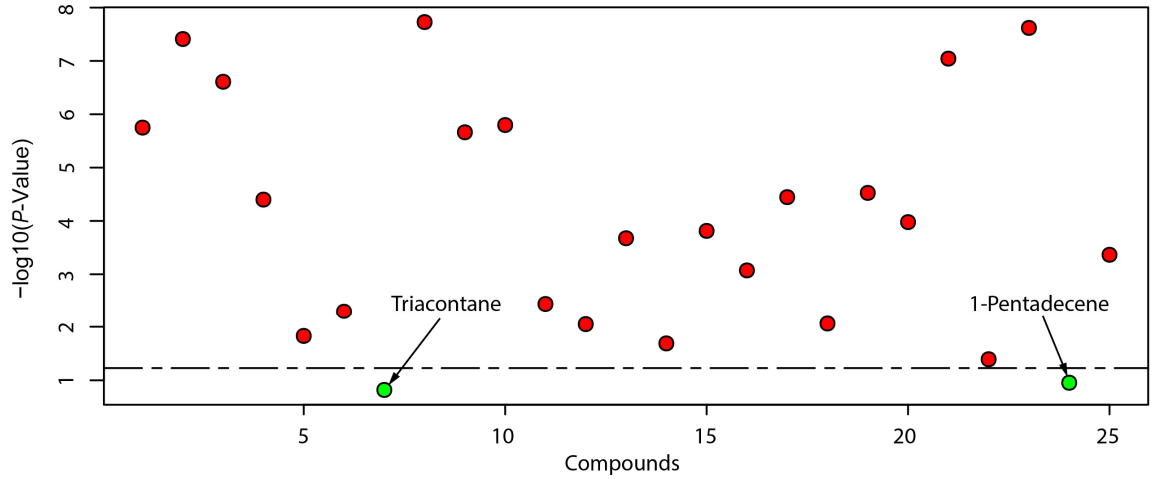

Figure 1. Metabolites obtained in control and EF treatment groups of *Tribolium castaneum* (Herbst). The points highlighted in red are significant compounds selected based on the *p*-value threshold (<0.05), and the green points represent nonsignificant compounds. Each point represents three biological replicates.

3.4. Hierarchical Cluster Analysis (HCA)

To better illustrate the differences and similarities in the metabolite concentrations between the control and EF treatment groups, the dataset was scaled using the heatmap package in R (v4.3.0), and the samples and metabolites were analyzed using a two-way cluster analysis. As shown in Figure 2a, each cell in the heatmap represents the concentration value of a metabolite, and the color scale from purple to red indicates the downregulation and upregulation of a metabolite, respectively. The heatmap provides a visual representation of the significant differences in the metabolic patterns of *T. castaneum* after the EF treatment, with strong similarities observed among the different PH_3-resistance levels. When we specifically focused on the resistance levels of adults of *T. castaneum*, these metabolites could, to a certain extent, identify the level of PH_3 resistance in both the treatment and control groups (Figure 2b,c). This finding is consistent with the results presented in Table 1.

Table 3. Profile of metabolites produced from different resistant levels of *Tribolium castaneum* (Herbst) between the treatment and control groups.

Metabolite	RT [1]	RI (*Exp*) [2]	RI (*Lit*) [3]	Relative Abundance (%) ± SD [5]						Log_2(FC)	*p*-Value (10^{-3})	CAS
				Con-S	Con-M	Con-SR	EF-S	EF-M	EF-SR			
2-Methyl-p-Benzoquinone	6.930	1028	1018	0.22 ± 0.01 ^{f}	0.45 ± 0.01 ^{e}	0.65 ± 0.03 ^{d}	0.92 ± 0.01 ^{c}	0.97 ± 0.01 ^{b}	1.27 ± 0.01 ^{a}	1.28	1.78×10^{-3}	553-97-9
2-Ethyl-p-Benzoquinone	8.915	1122	1215	0.42 ± 0.01 ^{f}	1.05 ± 0.06 ^{d}	0.81 ± 0.01 ^{e}	2.46 ± 0.17 ^{a}	1.41 ± 0.05 ^{c}	1.78 ± 0.25 ^{b}	1.30	3.88×10^{-5}	4754-26-1
Orcinol	13.666	1359	1374	1.45 ± 0.09 ^{a}	1.39 ± 0.11 ^{a}	1.16 ± 0.08 ^{b}	1.34 ± 0.08 ^{a}	1.33 ± 0.04 ^{a}	1.01 ± 0.04 ^{c}	−0.12	2.46×10^{-4}	504-15-4
2-Undecenal	14.126	1383	1367	N.D. [4] ^{b}	0.58 ± 0.03 ^{a}	0.56 ± 0.01 ^{a}	N.D. ^{b}	0.69 ± 0.01 ^{a}	0.67 ± 0.04 ^{a}	−0.058	3.98×10^{-2}	2463-77-6
Ethyl p-Hydroxybenzoate	15.212	1443	1438	1.89 ± 0.05 ^{bc}	3.28 ± 0.23 ^{c}	3.72 ± 0.17 ^{d}	1.94 ± 0.01 ^{abc}	3.16 ± 0.22 ^{a}	3.24 ± 0.55 ^{ab}	0.29	14.84	120-47-8
2-Dodecen-1-ol	16.09	1472	1472	0.97 ± 0.1 ^{b}	0.8 ± 0.09 ^{c}	1.08 ± 0.03 ^{b}	1.52 ± 0.05 ^{a}	1.08 ± 0.03 ^{b}	1.52 ± 0.23 ^{a}	0.49	5.04	22104-81-0
1-Pentadecene	16.491	1492	1515	21.3 ± 0.43 ^{ab}	21.55 ± 0.48 ^{ab}	19.84 ± 0.47 ^{b}	22.87 ± 2.45 ^{ab}	24.18 ± 2.3 ^{a}	22.66 ± 0.24 ^{ab}	0.16	53	13360-61-7
1-(2-Hydroxy-4-methoxyphenyl)propan-1-one	17.324	1564	1538 *	1.37 ± 0.03 ^{c}	2.15 ± 0.1 ^{c}	2.45 ± 0.04 ^{b}	1.62 ± 0.03 ^{b}	1.85 ± 0.09 ^{b}	2.92 ± 0.3 ^{a}	0.59	1.87×10^{-5}	6270-44-6
1-Hexadecene	18.079	1609	1592	0.76 ± 0.05 ^{d}	1.02 ± 0.09 ^{c}	0.95 ± 0.05 ^{c}	1.7 ± 0.06 ^{a}	1.43 ± 0.11 ^{b}	1.73 ± 0.3 ^{a}	0.82	2.18×10^{-3}	629-73-2
(Z,Z)-1,8,11-Heptadecatriene	19.252	1682	1665	0.78 ± 0.05 ^{c}	0.72 ± 0.1 ^{c}	0.72 ± 0.02 ^{c}	1.68 ± 0.12 ^{a}	1.25 ± 0.18 ^{b}	1.77 ± 0.24 ^{a}	1.07	1.59×10^{-3}	56134-03-3
(Z)-9-Tetradecen-1-ol	19.411	1691	1667	10.22 ± 0.87 ^{d}	12.21 ± 0.46 ^{c}	13.41 ± 1.12 ^{bc}	14.91 ± 1.13 ^{ab}	15.77 ± 0.85 ^{a}	14.2 ± 1.71 ^{abc}	0.35	3.61	35153-15-2
1-Hexadecanol	19.756	1714	1880	10.36 ± 0.30 ^{b}	10.17 ± 0.27 ^{b}	12.75 ± 0.43 ^{b}	13.52 ± 0.76 ^{a}	13.66 ± 1.60 ^{a}	10.36 ± 0.30 ^{a}	0.59	8.95	36653-82-4
Palmitic acid	23.762	1983	1968	1.78 ± 0.14 ^{c}	1.96 ± 0.12 ^{b}	1.91 ± 0.06 ^{bc}	2.99 ± 0.13 ^{a}	2.95 ± 0.2 ^{a}	3.01 ± 0.4 ^{a}	0.68	2.11×10^{-1}	66321-94-6
Alpha-linolenic acid	26.446	2160	2139	0.68 ± 0.1 ^{c}	0.78 ± 0.1 ^{bc}	0.87 ± 0.01 ^{a}	0.61 ± 0.05 ^{ab}	0.67 ± 0.02 ^{a}	1.09 ± 0.26 ^{ab}	0.56	20.495	463-40-1
Oleic acid	26.801	2184	2141	1.77 ± 0.15 ^{c}	2 ± 0.02 ^{bc}	1.43 ± 0.08 ^{ab}	2.08 ± 0.12 ^{c}	2.34 ± 0.24 ^{c}	2.53 ± 0.28 ^{a}	0.0064	1.54×10^{-1}	112-80-1
Tricosane	31.872	2337	2300	1.4 ± 0.23 ^{a}	0.38 ± 0.04 ^{c}	0.29 ± 0.03 ^{c}	1.32 ± 0.54 ^{b}	N.D. ^{c}	N.D. ^{c}	1.09	8.46×10^{-1}	638-67-5
Pentacosane	33.426	2369	2500	1.82 ± 0.2 ^{ab}	2.32 ± 0.24 ^{a}	1.72 ± 0.13 ^{ab}	1.65 ± 0.12 ^{c}	1.21 ± 0.12 ^{bc}	1.54 ± 0.41 ^{ab}	−0.51	3.58×10^{-2}	629-99-2
11-Methylheptacosane	34.422	2489	2535	2.26 ± 0.035 ^{c}	2.65 ± 0.021 ^{a}	2.48 ± 0.064 ^{b}	2.19 ± 0.056 ^{c}	2.03 ± 0.035 ^{d}	2.46 ± 0.10 ^{b}	−0.16	1.05×10^{-1}	15689-68-6
Hexacosane	34.634	2704	2600	2.48 ± 0.18 ^{b}	2.8 ± 0.23 ^{b}	2.84 ± 0.33 ^{b}	1.84 ± 0.11 ^{a}	2.06 ± 0.15 ^{a}	1.9 ± 0.12 ^{a}	−0.25	8.70	630-01-3
13-Methylheptacosane	35.561	2721	2731	0.65 ± 0.03 ^{a}	0.58 ± 0.06 ^{ab}	0.5 ± 0.06 ^{bc}	0.6 ± 0.05 ^{a}	0.47 ± 0.04 ^{c}	0.4 ± 0.05 ^{d}	−0.070	2.98×10^{-2}	15689-72-2
Octacosane	36.083	2731	2800	6.96 ± 0.49 ^{a}	6.94 ± 0.46 ^{a}	7.4 ± 0.85 ^{a}	3.78 ± 0.37 ^{b}	3.75 ± 0.31 ^{b}	3.52 ± 0.59 ^{b}	−0.81	9.05×10^{-5}	630-02-4
Nonacosane	37.352	2755	2900	N.D. ^{c}	0.98 ± 0.02 ^{bc}	1.09 ± 0.01 ^{bc}	1.88 ± 0.2 ^{a}	1.42 ± 0.07 ^{b}	1.99 ± 0.29 ^{a}	0.78	40.506	630-03-5
15-Methylnonacosane	37.921	2766	2923	3.17 ± 0.27 ^{bc}	3.29 ± 0.33 ^{a}	3.31 ± 0.17 ^{b}	2.89 ± 0.16 ^{c}	2.41 ± 0.12 ^{d}	2.4 ± 0.29 ^{d}	−0.51	2.40×10^{-5}	65820-60-2
Triacontane	38.276	2772	3000	3.35 ± 0.22 ^{a}	3.37 ± 0.24 ^{a}	3.55 ± 0.35 ^{a}	3.37 ± 0.26 ^{a}	3.7 ± 0.17 ^{a}	3.95 ± 0.014 ^{a}	0.085	133	638-68-6
Lathosterol	40.392	3320	3170	2.63 ± 0.11 ^{b}	2.67 ± 0.44 ^{b}	2.22 ± 0.2 ^{b}	3.78 ± 0.27 ^{a}	4.0 5 ± 0.27 ^{a}	4.27 ± 0.6 ^{a}	0.68	4.31×10^{-1}	80-99-9

[1] RT: Retention time. [2] RI(*Exp*): Retention Index determined by using n-alkane standard C7-C40. [3] RI(Lit): Standard of Retention Index from NIST Library. [4] N.D.: Not detected. [5] SD: Standard deviation. * Estimated non-polar retention index (n-alkane scale NIST). Values represent the means of three replicates, and values within the same row with different superscript letters are significantly different ($p < 0.05$).

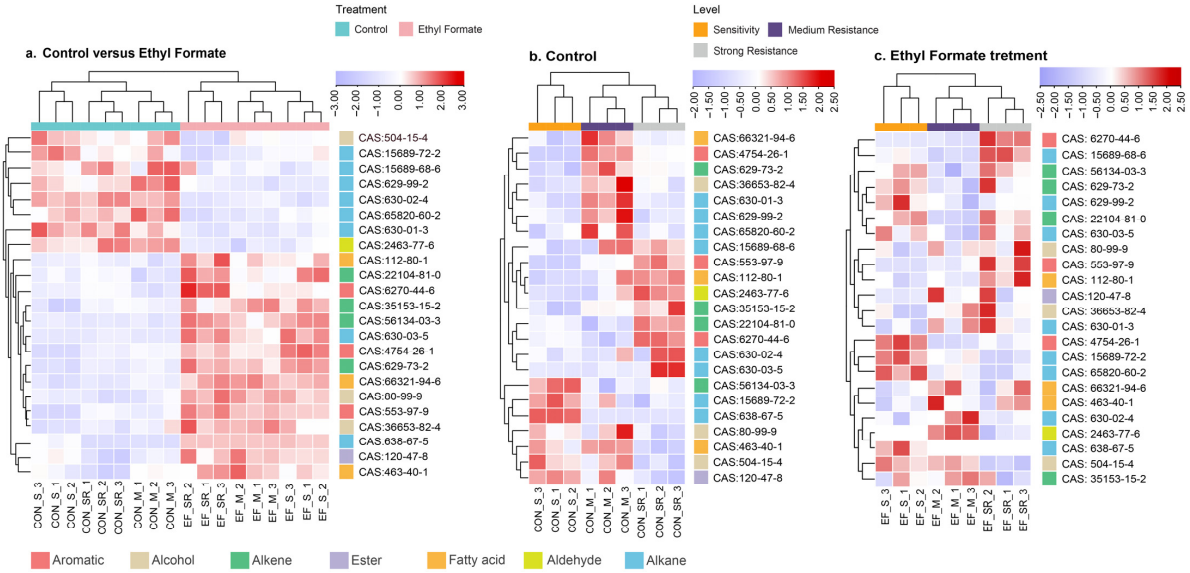

Figure 2. Clustering heatmap analysis. The left heatmap (**a**) shows differentially abundant metabolite modules between ethyl formate treatment and the control group (**b**), and the right heatmap (**c**) shows the different phosphate-resistant levels in relation to the control group.

3.5. Artificial Neural Network (ANN)

To describe the relationship between the above 23 compounds and *T. castaneum* exhibiting different PH_3 resistance levels before and after the EF treatment more accurately, we used the ANN tool in MATLAB to build a recognition model (Figure 3). The constructed network model was a two-layer feedforward network with a sigmoid transfer function in the hidden layer and a softmax transfer function in the output layer. The sigmoid function maps the input values to the interval (0, 1), whereas the softmax function normalizes the output values into probability measures in the metric space. The final count of neurons in the hidden layer was established as six, which was determined through a trial-and-error approach and selection based on methods, such as cross-validation. To train the multilayer feedforward network, a scaled conjugate gradient (trainscg) numerical optimization algorithm was employed to optimize the performance functions. A cross-entropy function was introduced into the training process to measure the difference in the probability distribution. A smaller cross-entropy indicates higher classification accuracy, and the training process automatically stops when neural network optimization reaches a certain level [29].

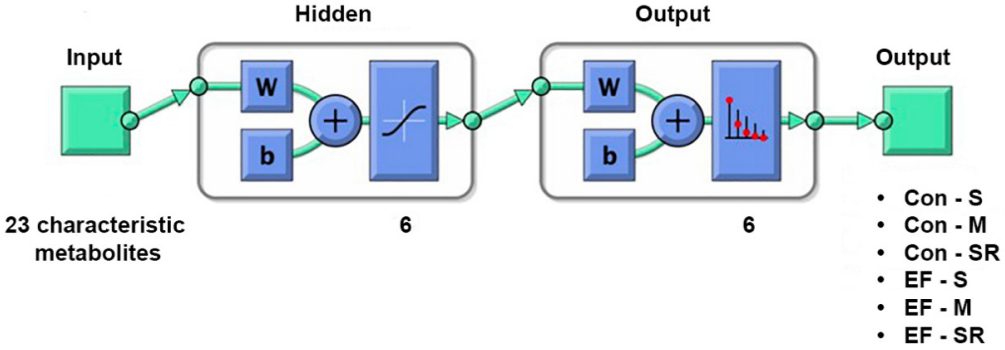

Figure 3. The architecture of the Artificial Neural Network (ANN) model constructed from the DI-SPME-GCMS metabolite profiles of *Tribolium castaneum* (Herbst) with different levels of PH_3 resistance in both EF-treated and untreated groups. W and b are the network's adjustable parameters, representing the weight matrices and bias vectors, respectively. Once the network is trained, its bias and weight values form into a vector. This single vector is then redivided into the original biases and weights.

Data processing is vital for training neural networks because it directly affects the predictive accuracy of the model. All recognition tasks were performed using the ANN model based on the metabolite data, and the data were assigned to one of the following groups: Con-S, Con-M, Con-SR, EF-S, EF-M, or EF-SR. Once the network training was completed, its performance was evaluated using cross-entropy (where lower values signify greater accuracy) and the percentage of misclassification errors. The results were analyzed using a visualization tool with confusion matrices (Figure 4). The ANN model, trained with 66.67% of the randomly assigned metabolite data (12 samples), achieved 100% accuracy in identification, as illustrated in Figure 4a. In the validation of the trained model, using 16.67% of the randomly assigned metabolite data (three samples) resulted in the precise identification of all *T. castaneum* groups (Figure 4b). The testing set consisting of 16.67% randomly assigned data (three samples) yielded 66.67% correct identifications, as shown in Figure 4c. Overall, the developed ANN model achieved a classification accuracy of 94.4% (Figure 4d). It was able to accurately identify the metabolite dataset from the Con-S, Con-M, Con-SR, EF-M, and EF-SR groups (100%) and achieved 66.67% accuracy for the EF-S group [30]. Therefore, it was reasonable to use these 23 metabolites as a dataset of interest to study the toxicological mechanisms of EF in adult *T. castaneum* strains with different levels of PH_3 resistance.

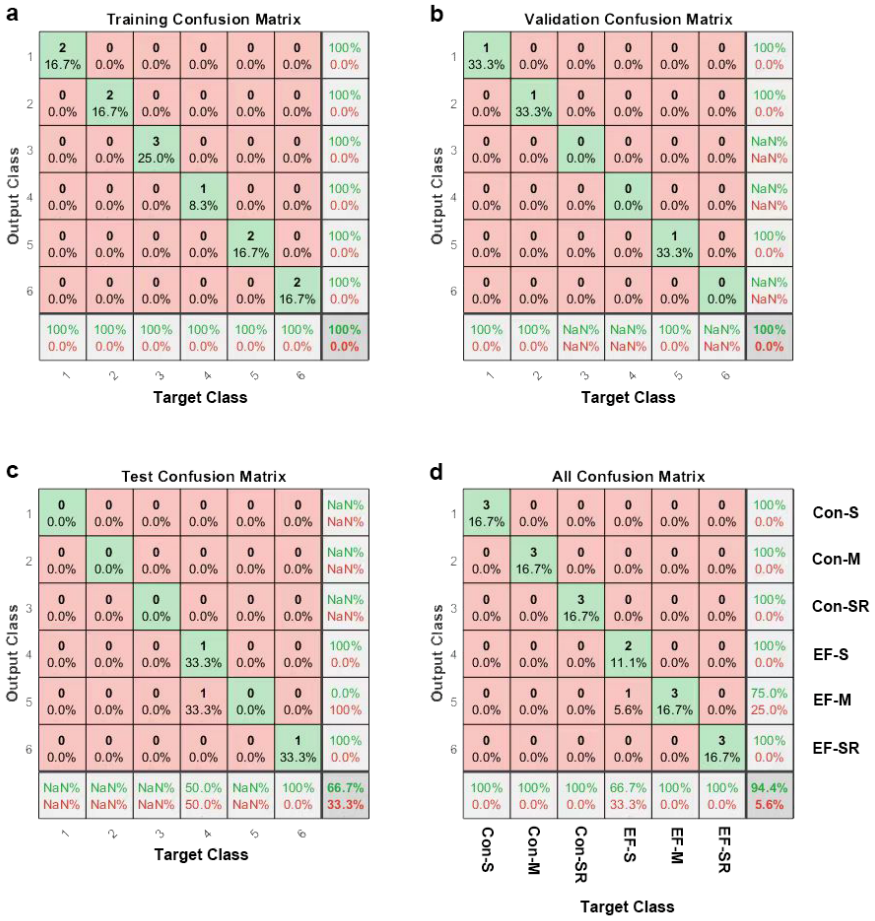

Figure 4. Confusion matrices displaying the overall accuracy and errors in classifications. The green squares along the diagonal of the matrix indicate correct classifications, while the red squares show where misclassifications have occurred. Each cell box provides the count and proportion of the *Tribolium castaneum* (Herbst) samples. A well-performing network is characterized by lower percentages in the red squares, signifying minimal misclassifications. Different sets of confusion matrices are presented as follows: (**a**) training set, (**b**) validation set, (**c**) testing set, and (**d**) all confusion matrices in one matrix.

3.6. Multivariate Statistical Analysis of Metabolites in T. castaneum after EF Fumigation

A multivariate statistical analysis simplifies and reduces the dimensionality of high-dimensional and complex data while retaining the wealth of the original information [31]. A PCA is an unsupervised method that provides an overall summary of the clustering information among groups without sample designation. The grouping in the PCA score plot was based on similarities between the metabolic profiles of the samples. The PCA results reveal a distinct separation between the EF treatment group and the control group along the first principal component (PC1), explaining 59.43% of the total variance. Moreover, there is a non-overlapping 95% Hotelling's T-squared ellipse between the EF treatment group and the control group (Figure 5a).

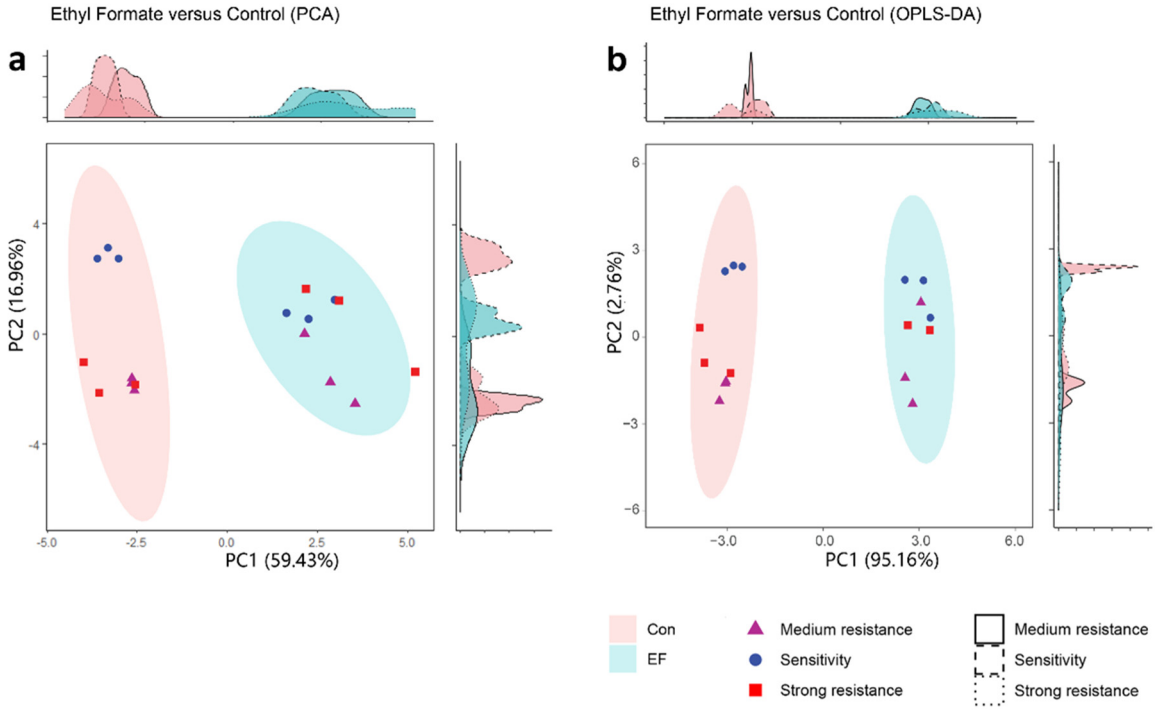

Figure 5. Principal Component Analysis (PCA) (**a**) and Orthogonal Projections to Latent Structures Discriminant Analysis (OPLS-DA) (**b**) indicate a significant separation between treatment with ethyl formate and controls for metabolome. These changes are not associated with phosphine resistance levels. The reliability of the OPLS-DA model was determined using a permutational test.

An OPLS-DA is a multidimensional statistical analysis method used for supervised pattern recognition. Compared with a PCA, an OPLS-DA not only achieves dimensionality reduction but also considers grouping information, which means that an OPLS-DA can remove orthogonal variables from metabolites that are unrelated to category variables, providing more accurate distinctions between metabolites. The score plot in Figure 5b clearly shows a significant separation between the EF treatment and control groups, with the treatment group located on the right side and the control group on the left side. Meanwhile, no outlier samples existed within the treatment and control groups (outside the 95% Hotelling's T-squared ellipse) in the OPLS-DA model, indicating that the OPLS-DA model enabled a more significant tendency for sample clustering within each group compared to the PCA model. These results demonstrate that EF treatment affected the metabolic profile of *T. castaneum* at different resistance levels.

Furthermore, within the PCA model and OPLS-DA, samples of *T. castaneum* with varying levels of PH_3 resistance exhibited relatively dispersed distributions within each group (excluding TC-S). This observation suggests that EF treatment does not alter the metabolic characteristics associated with PH_3 resistance, particularly in resistant strains (TC-M and TC-SR). For the susceptible strain, EF treatment influenced the expression of

certain compounds in its metabolite profile, thereby eliminating the differences between the susceptible and resistant strains. This can be attributed to relatively minor changes in potential PH_3 resistance biomarkers, thus eliminating distinctions among *T. castaneum* strains with varying PH_3 resistance levels within the EF treatment group.

3.7. Screening and Analysis of Differentially Regulated Metabolites in T. castaneum after Treatment with EF

"Differential metabolites" refer to the substances found in two samples that show significant quantitative differences. The metabolites responsible for the separation were determined based on VIP values (≥1) [32]. As shown in Figure 6a, a comparison between the control and EF treatment groups identified 11 differential metabolites, with two metabolites downregulated in abundance following the EF treatment (including 15-Methylnonacosane (CAS: 65820-60-2 and CAS: 4754-26-1) and octacosane (CAS: 630-02-4)). A volcano plot analysis (Figure 6b) identified 12 metabolites that met the criteria for feature selection ($p \leq 0.05$ and Log_2(FoldChange) ≥ 0.5). This analysis excluded features with low potential biological relevance (characterized by minimal between-class differences) to prevent their selection based on negligible within-class variation. Among the metabolites independently selected using the two methods, eleven were identified (Table 4), including two fatty acids, two alcohols, two alkenes, three alkanes, and two aromatics. Furthermore, the relative abundance of most of these differential metabolites was upregulated after the EF treatment.

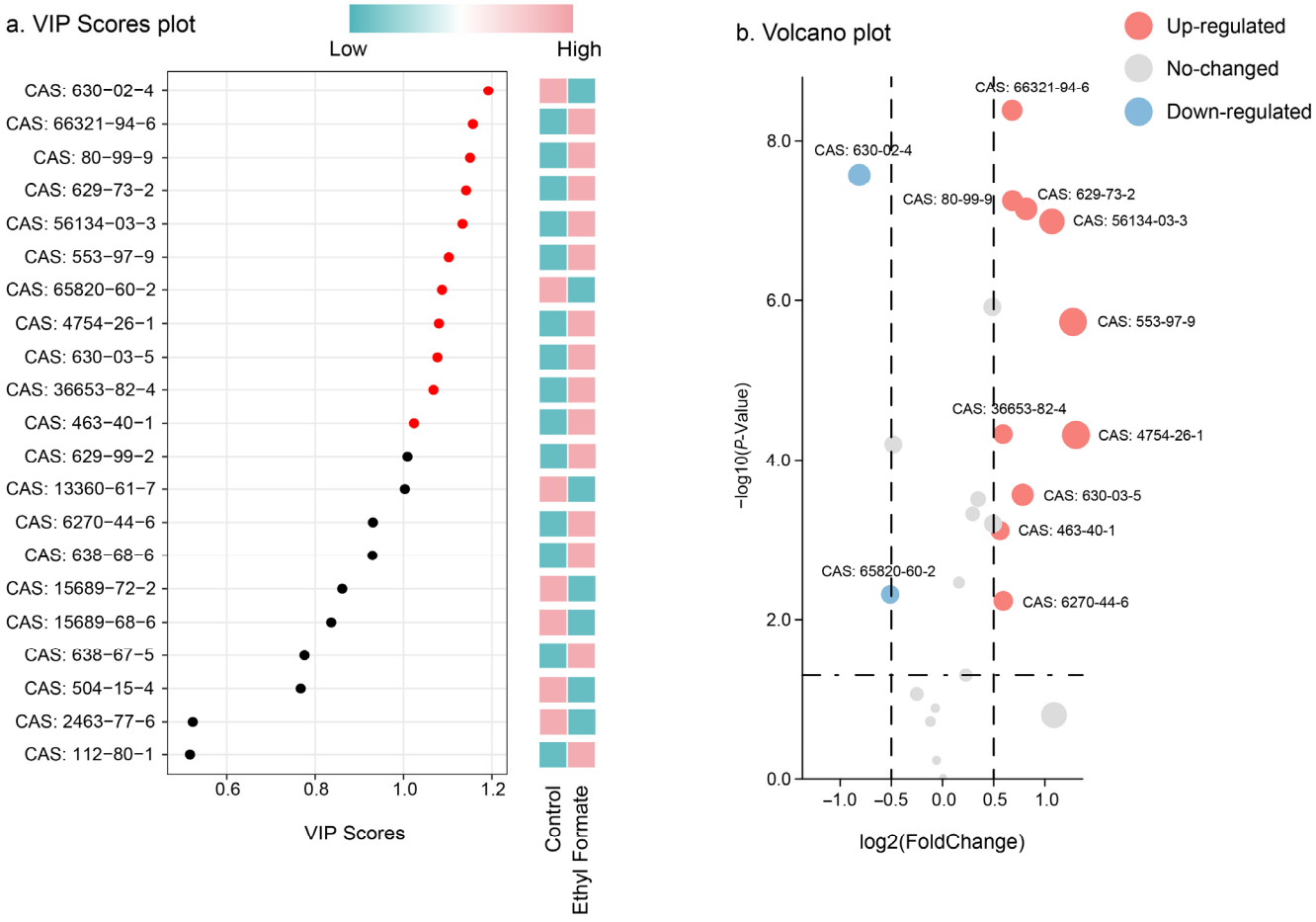

Figure 6. Variable importance projection (VIP) scores from OPLS-DA analysis of adult *Tribolium castaneum* (Herbst) samples showing eleven significantly different metabolites between the control and EF treatment groups (**a**). Volcano plot of significantly upregulated (red) and downregulated (blue) metabolites ($p \leq 0.05$ and $|Log_2(FoldChange)| \geq 0.5$) (**b**).

Table 4. Identification of differentially abundant metabolites in DI-SPME coupled with GC-MS between the ethyl formate treatment and control groups.

Classification	Metabolite (CAS Number)	VIP Score [1]	*p*-Value [2]	FDR [3]	Log_2(Fold Change)	Regulation
Fatty acid	Palmitic acid (CAS: 66321-94-6)	1.27625	4.17×10^{-9}	4.17×10^{-9}	0.68	Up
	Alpha-linolenic acid (CAS: 463-40-1)	1.0192	7.69×10^{-4}	1.75×10^{-3}	0.56	Up
Alcohol	Lathosterol (CAS: 80-99-9)	1.2758	5.61×10^{-8}	6.10×10^{-8}	0.68	Up
	1-Hexadecanol (CAS: 36653-82-4)	1.13047	4.69×10^{-5}	6.52×10^{-5}	0.59	Up
Alkene	1-Hexadecene (CAS: 629-73-2)	1.26547	7.13×10^{-8}	8.10×10^{-8}	0.82	Up
	(Z,Z)-1,8,11-Heptadecatriene (CAS: 56134-03-3)	1.26488	1.02×10^{-7}	1.21×10^{-7}	1.07	Up
Alkane	Octacosane (CAS: 630-02-4)	1.31529	2.65×10^{-8}	2.76×10^{-8}	−0.81	Down
	15-Methylnonacosane (CAS: 65820-60-2)	1.14394	4.88×10^{-3}	1.36×10^{-2}	−0.51	Down
	Nonacosane (CAS: 630-03-5)	1.13624	2.76×10^{-4}	4.59×10^{-4}	0.78	Up
Aromatic	2-Methyl-p-Benzoquinone (CAS: 553-97-9)	1.19573	1.85×10^{-6}	2.43×10^{-6}	1.28	Up
	2-Ethyl-p-Benzoquinone (CAS: 4754-26-1)	1.13628	4.80×10^{-5}	7.05×10^{-5}	1.30	Up

[1] VIP Score: Variable importance in projection score from the OPLS-DA model. [2] *p*-value: Student's *t*-test *p*-value. [3] FDR: Corrected *p*-value using the Benjamini−Hochberg method.

3.8. Key Metabolic Pathway Preliminary Analysis

Two types of enrichment analyses were performed using R software. The ClusterProfiler packages from BioConductor were used. The enrichment analysis provided a pair of bar graphs and bubble plots.

A bubble plot (Figure 7a) and bar graph (Figure 7b) were constructed using the high-quality KEGG metabolic pathway database as the back-end knowledge base. Compounds that were differentially expressed between the EF treatment and control groups were enriched in six metabolic pathways. Based on the *p*-value and impact values, two pathways were identified as the key responsive pathways to the EF treatment of *T. castaneum* adults. These pathways included fatty acid degradation and the biosynthesis of unsaturated fatty acids, with impact values of 0.0655 and 0.097, respectively.

3.9. Comparison of the Key Differential Metabolic Responses

To better understand the metabolic responses induced by the EF treatment *in T. castaneum*, we integrated key metabolic pathways (Figure 7a,b) and their corresponding differentially regulated metabolites (Table 5), which were identified through multivariate and univariate statistical analyses based on the KEGG and MetaCyc databases. A schematic network of metabolic pathways was constructed using this information (Figure 8).

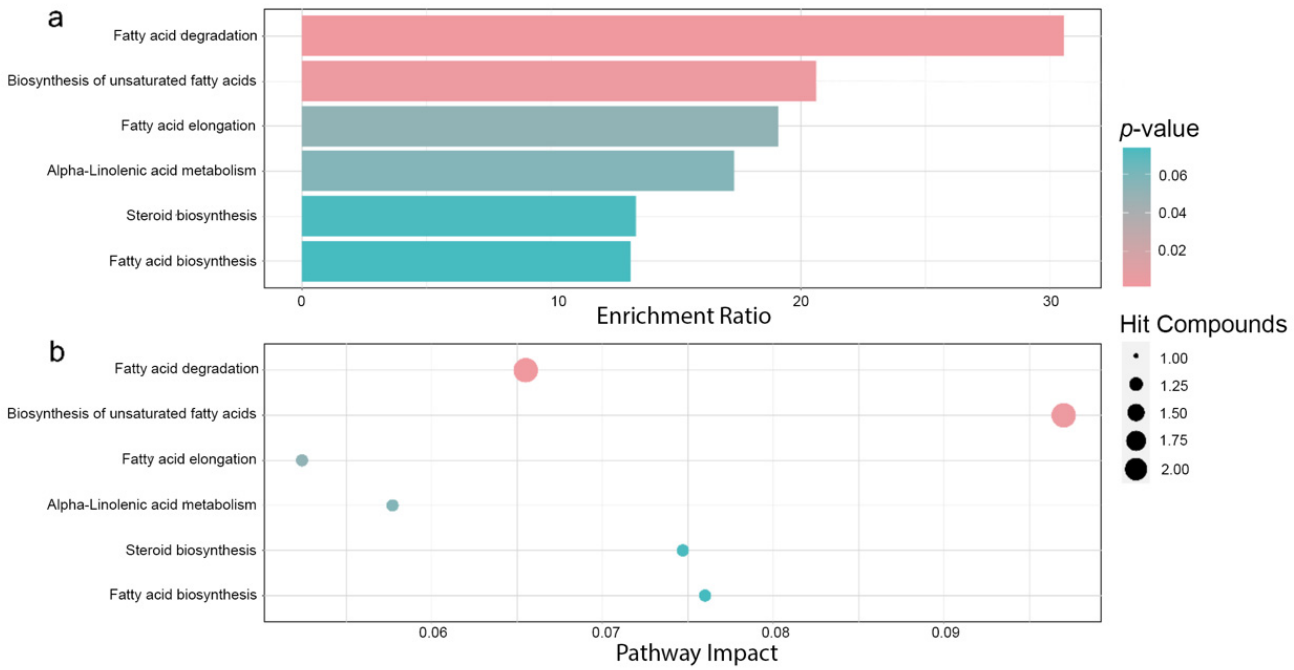

Figure 7. KEGG enrichment analysis of 11 differential metabolites (VIP $\geq$ 1, $p \leq 0.05$, and Log_2(FoldChange) $\geq$ 0.5) in *Tribolium castaneum* (Herbst) with ethyl formate treatment. The results were visualized using a bar plot and bubble diagram. Bar plot: Gradients of colors are based on the *p*-value (**a**). Bubble plot: Gradients of colors are based on the *p*-value. The size of the circle represents the hit compounds (**b**).

Table 5. Pathway analysis results from the adults of *Tribolium castaneum* (Herbst) metabolomics for ethyl formate treatment group versus control group.

Pathway	Total	Hit Compounds	*p*-Value	Holm P	Impact
Fatty acid degradation	50	Palmitic acid, 1-hexadecanol	0.00155	0.138	0.0655
Biosynthesis of unsaturated fatty acids	74	Palmitic acid, Alpha-linolenic acid	0.00337	0.297	0.097
Fatty acid elongation	40	Palmitic acid	0.0514	1	0.0524
Alpha-linolenic acid metabolism	44	Alpha-linolenic acid	0.0565	1	0.0577
Steroid biosynthesis	57	Lathosterol	0.0727	1	0.0747
Fatty acid biosynthesis	58	Palmitic acid	0.0739	1	0.076

As shown in Figure 8, a schematic of the key metabolic pathways represents the major differential metabolic routes significantly influenced by EF in adult *T. castaneum*, with six key metabolic pathways corresponding to the four differentially regulated metabolites. The schematic network shows that palmitic acid and 1-hexadecanol correspond to fatty acid degradation; palmitic acid and alpha-linolenic acid correspond to the biosynthesis of unsaturated fatty acids; alpha-linolenic acid corresponds to alpha-linolenic acid metabolism; lathosterol corresponds to steroid biosynthesis; and palmitic acid corresponds to both fatty acid biosynthesis and elongation. Fatty acid degradation and the biosynthesis of unsaturated fatty acids are significant responses of *T. castaneum* adults to EF.

Overall, the metabolomics data provide evidence that strongly suggests that EF treatment has a significant impact on the fatty acid metabolic pathways of adult *T. castaneum*, with the primary loci of action being the mitochondria and endoplasmic reticulum. Specifically, EF stimulation increased the levels of these four key compounds in the aforementioned metabolic pathways. Notably, these changes were not related to PH_3 resistance in *T. castaneum*.

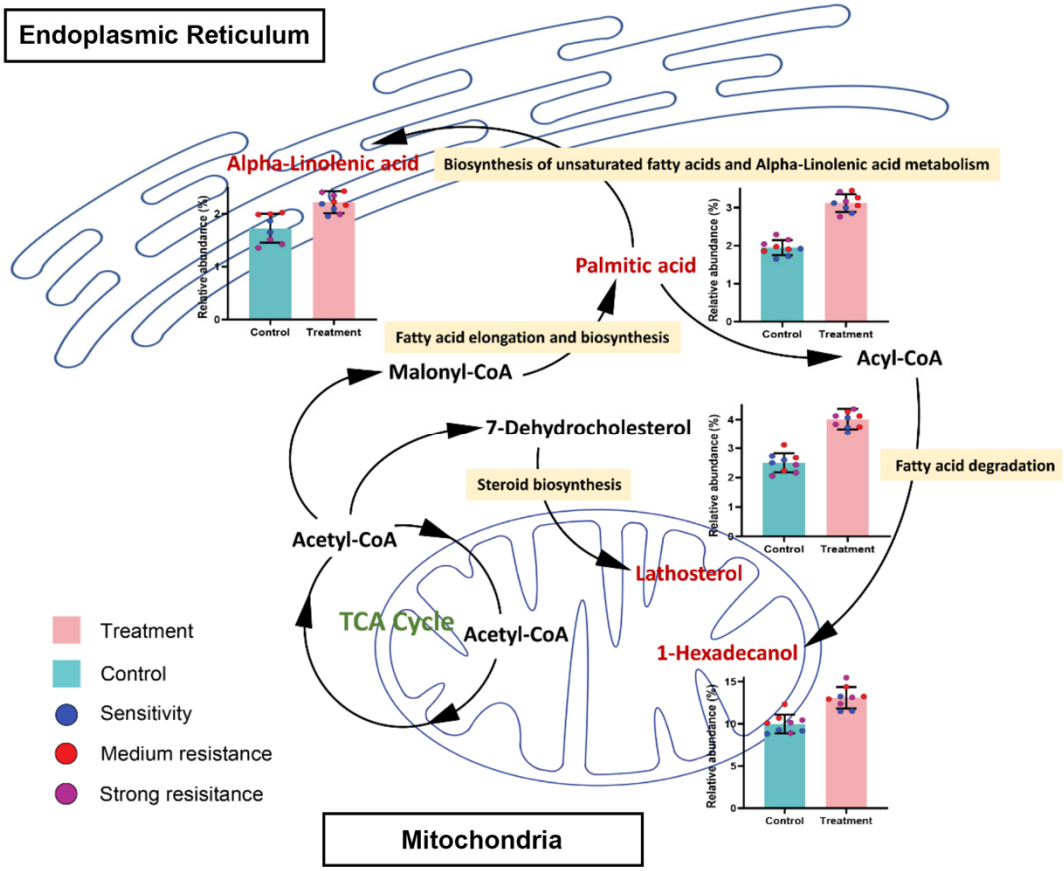

Figure 8. Schematic network of the identified lipid metabolism pathways in the ethyl formate treatment group of *Tribolium castaneum* (Herbst).

4. Discussion

Given that phosphine (PH_3) is currently the most widely used registered grain fumigant in the world, and with the emergence of strongly PH_3-resistant pests, increased research attention has been paid to the toxicity mechanism of the potential alternative fumigant ethyl formate (EF). This study explored the toxic effects of EF on various PH_3-resistant *T. castaneum* models. We found that EF exhibited significant toxicity even in *T. castaneum* strains that are highly resistant to PH_3. This observation suggests that there may not be a direct correlation between the toxic action of EF and resistance mechanisms against PH_3.

In the present study, we conducted a comparative analysis of the tolerance responses of three strains of *T. castaneum* adults to PH_3 and EF. Our results, based on the LC_{50} and LC_{99} levels, identified moderate susceptibility and strong levels of PH_3 resistance among the three strains. Interestingly, despite varying levels of resistance to PH_3, the responses of the different *T. castaneum* strains to EF were similar (TC-S: LC_{99} = 25.970; TC-M: LC_{99} = 24.797; and TC-SR: LC_{99} = 25.146). This suggests that the differential susceptibility can be attributed to the fundamental differences in the chemical properties of EF and PH_3 [23]. Further research into the response of *T. castaneum* to EF has revealed complex biochemical regulations. Specifically, using DI-SPME and GC-MS, we observed significant changes in 23 compounds in *T. castaneum* treated with EF. These metabolic changes are related to alterations in lipid metabolism, enhanced lipid peroxidation, and the activation of the antioxidant enzyme system. This suggests that EF toxicity acts through the induction of oxidative stress and the disruption of normal lipid metabolism. These alterations, confirmed through an HCA and ANN analysis, effectively differentiated the EF-treated group from the control group, providing support for subsequent metabolomic analyses. Additionally, we noted an interesting correlation: the variation in the content of 2-methyl-p-benzoquinone positively correlated with the PH_3 resistance of *T. castaneum*

adults in both the treated and control groups, indicating that 2-methyl-p-benzoquinone could potentially serve as an ideal biomarker for identifying the levels of PH_3 resistance in *T. castaneum* and possibly other insect species.

An analysis of enrichment and metabolic pathways showed that the differential compounds produced at different PH_3 resistance levels in *T. castaneum* adults after the EF treatment were related to the lipid pathway. We found that fatty acid synthesis (the biosynthesis of unsaturated fatty acids, fatty acid elongation, fatty acid biosynthesis, and alpha-linolenic acid metabolism), fatty acid β-oxidation (fatty acid degradation), and steroid biosynthesis pathways were affected, and EF had the most significant effect on fatty acid degradation.

Palmitic acid is an EF-specific, differentially regulated metabolite in *adult T. castaneum*. It is an important saturated fatty acid that can further enhance oxidative stress in cells by damaging the normal function of the mitochondrial respiratory chain, resulting in damage to fatty acid degradation and the accumulation of fatty acids in the cytoplasm [33,34]. Palmitic acid induces a surge in reactive oxygen species (ROS) levels and causes apoptosis. Excessive ROS production can disrupt the balance between cellular oxidation and the antioxidant system [35]. In this study, we found that the relative palmitic acid content increased in *T. castaneum* adults treated with EF. Palmitic acid has been widely reported as a signaling molecule for intracellular oxidative stress, and an increased palmitic acid content has been detected in cells injured by ROS accumulation and lipid peroxidation [36,37]. These studies indicated that the toxicological mechanism of EF is similar to that of PH_3, leading to death through indirect physiological effects on the aerobic respiration of insects.

Alpha-linolenic acid is another specific differential metabolite that increases in *T. castaneum* adults following EF treatment, and it plays key roles in insect growth, development, and tolerance to abiotic stress [38]. Similar to palmitic acid, alpha-linolenic acid triggers apoptosis by increasing the ROS levels and enhancing lipid peroxidation. 1-Hexadecanol, a reduction product of palmitic acid and a vital intermediary in fatty acid beta-oxidation, exhibited increased levels, indicating potential interference by EF in the fatty acid degradation process. Lathosterol, a sterol related to insect growth and development that is catalyzed by the cytochrome P450 enzyme family, consumes a significant amount of ATP during its synthesis and modification [39,40]. Thus, the higher lathosterol content observed after the EF treatment supports the hypothesis that EF affects the fatty acid degradation pathway. Furthermore, the disruption of beta-oxidation by steroids leads to an insufficient supply of acetyl-CoA, potentially affecting the tricarboxylic acid cycle and fatty acid synthesis pathways [41,42]. Additionally, the role of cytochrome P450 enzymes (CYPs) in *T. castaneum*'s metabolism of EF should be considered. Although the function of CYP enzymes in this process remains unclear, their impact seems to diverge significantly from their known role in the development of PH_3 resistance [43,44]. This is consistent with the findings of Kim et al., who suggested that insects can adapt to various environmental stresses through multiple complex biochemical pathways [13]. Although the enrichment analysis did not indicate a significant impact on these pathways, this may be a result of the associated response caused by metabolic pathways significantly affected by EF rather than a direct effect of EF on fatty-acid-synthesis-related pathways.

In conclusion, the differences in the toxicological mechanisms of EF and the resistance mechanisms to PH_3 offer a potential pathway for designing alternative fumigants that are capable of overcoming existing fumigant resistance. Therefore, when developing new pest control strategies, it is essential to consider the unique responses of insects to different fumigants. These studies suggest that, although the toxicological mechanisms of EF and PH_3 share similarities, particularly in terms of inhibiting respiration by damaging the mitochondria, our experiments demonstrated that *T. castaneum* strains with varying levels of PH_3 resistance do not exhibit cross-resistance to EF [12,45,46]. This variation in mechanisms enables EF to effectively target PH_3-resistant insects. Our preliminary research on the toxicological mechanism of EF, conducted using DI-SPME and GC-MS analysis, highlights the significance of EF-induced beta-oxidation damage to fatty acids, leading to

cellular lipotoxicity. Future research should explore, in greater depth, the action mechanism of EF on *T. castaneum* and other PH_3-resistant pests from proteomic and enzymological perspectives, validating each potential biomarker for a more comprehensive understanding of the toxicological mechanism of EF.

Author Contributions: Conceptualization, C.S. and T.L.; Methodology, C.S., X.D. and Y.R.; Software, C.S.; Validation, C.S.; Formal Analysis, C.S.; Investigation, C.S. and T.L.; Resources, C.S. and X.Y.; Data Curation, C.S. and L.L.; Writing—Original Draft, C.S.; Writing—Review and Editing, C.S., Y.R. and T.L.; Visualization, C.S.; Supervision, T.L.; Project Administration, Y.R. and T.L.; Funding Acquisition, T.L. All authors have read and agreed to the published version of the manuscript.

Funding: This research was funded by the Beijing Natural Science Foundation (No. 6212032) and the technical support fund for the postharvest control of biological contaminants of the State Administration for Market Regulation (No. 2024).

Institutional Review Board Statement: The study was conducted according to the guidelines of the Declaration of Helsinki and was approved by Chinese Academy of Inspection and Quarantine (Approval Code: 2023S003, and Approval Date: 13 September 2023).

Data Availability Statement: All data are contained within the article.

Conflicts of Interest: The authors declare no conflicts of interest.

References

1. Hasan, M.; Aikins, M.; Schilling, M.; Phillips, T. Comparison of methyl bromide and phosphine for fumigation of *Necrobia rufipes* (Coleoptera: Cleridae) and *Tyrophagus putrescentiae* (Sarcoptiformes: Acaridae), pests of high-value stored products. *J. Econ. Entomol.* **2020**, *113*, 1008–1014. [CrossRef]
2. Konemann, C.; Hubhachen, Z.; Opit, G.; Gautam, S.; Bajracharya, N. Phosphine resistance in *Cryptolestes ferrugineus* (Coleoptera: Laemophloeidae) collected from grain storage facilities in Oklahoma, USA. *J. Econ. Entomol.* **2017**, *110*, 1377–1383. [CrossRef]
3. Porter, I.; Banks, J.; Mattner, S.; Fraser, P. Global phaseout of methyl bromide under the Montreal protocol: Implications for bioprotection, biosecurity and the ozone layer. In *Recent Developments in Management of Plant Diseases*; Spring: Berlin/Heidelberg, Germany, 2009; pp. 293–309.
4. Cao, Y.; Wang, D. Relationship between phosphine resistance and narcotic knockdown in *Tribolium castaneum* (Herbst), *Sitophilus oryzae* (L.), and *S. zeamais* (Motsch). In Proceedings of the Conference Controlled Atmosphere and Fumigation in Stored-Products 2020, Adelaide, Australia, 1–4 August 2020; pp. 1–4.
5. Walter, G.H.; Chandrasekaran, S.; Collins, P.J.; Jagadeesan, R.; Mohankumar, S.; Alagusundaram, K.; Subramanian, S. The grand challenge of food security-general lessons from a comprehensive approach to protecting stored grain from insect pests in Australia and India. *Indian J. Entomol.* **2016**, *78*, 7–16. [CrossRef]
6. Jagadeesan, R.; Nayak, M.K. Phosphine resistance does not confer cross-resistance to sulfuryl fluoride in four major stored grain insect pests. *Pest Manag. Sci.* **2017**, *73*, 1391–1401. [CrossRef]
7. Chiluwal, K.; Lee, B.H.; Kwon, T.H.; Kim, J.; Park, C.G. Post-fumigation sub-lethal activities of phosphine and ethyl formate on survivorship, fertility and female sex pheromone production of *Callosobruchus chinensis* (L.). *Sci. Rep.* **2023**, *13*, 4333. [CrossRef]
8. Xin, N.; Ren, Y.L.; Forrester, R.I.; Ming, X.; Mahon, D. Toxicity of ethyl formate to adult *Sitophilus oryzae* (L.), *Tribolium castaneum* (herbst) and *Rhyzopertha dominica* (F.). *J. Stored Prod. Res.* **2008**, *44*, 241–246. [CrossRef]
9. Ren, Y.; Lee, B.; Padovan, B.; Cai, L. Ethyl formate plus methyl isothiocyanate—A potential liquid fumigant for stored grains. *Pest Manag. Sci.* **2012**, *68*, 194–201. [CrossRef]
10. Kim, B.; Song, J.E.; Park, J.S.; Park, Y.; Shin, E.M.; Yang, J. Insecticidal effects of fumigants (EF, MB, and PH_3) towards phosphine-susceptible and-resistant *Sitophilus oryzae* (Coleoptera: Curculionidae). *Insects* **2019**, *10*, 327. [CrossRef] [PubMed]
11. Deng, Y.X.; Wang, J.J.; Dou, W.; Yang, Z.L.; Jiang, T.K. Fumigation activities of ethyl formate on different strains of *Liposcelis bostrychophila*. *Jul.-Kühn-Arch.* **2010**, *425*, 459–463.
12. Haritos, V.S.; Dojchinov, G. Cytochrome c oxidase inhibition in the rice weevil *Sitophilus oryzae* (L.) by formate, the toxic metabolite of volatile alkyl formates. *Comp. Biochem. Physiol. Part C Toxicol. Pharmacol.* **2003**, *136*, 135–143. [CrossRef] [PubMed]
13. Kim, K.; Yang, J.O.; Sung, J.Y.; Lee, J.Y.; Park, J.S.; Lee, H.S.; Lee, S.E. Minimization of energy transduction confers resistance to phosphine in the rice weevil, *Sitophilus oryzae*. *Sci. Rep.* **2019**, *9*, 14605.
14. Kim, K.; Lee, Y.H.; Kim, G.; Lee, B.H.; Yang, J.O.; Lee, S.E. Ethyl formate and phosphine fumigations on the two-spotted spider mite, *Tetranychus urticae* and their biochemical responses. *Appl. Biol. Chem.* **2019**, *62*, 50. [CrossRef]
15. Alnajim, I.; Du, X.; Lee, B.; Agarwal, M.; Liu, T.; Ren, Y. New method of analysis of lipids in *Tribolium castaneum* (Herbst) and *Rhyzopertha dominica* (Fabricius) insects by direct immersion solid-phase microextraction (DI-SPME) coupled with GC–MS. *Insects* **2019**, *10*, 363. [CrossRef]

16. Li, L.; Shan, C.; Liu, Q.; Li, B.; Liu, T. Comparative Analysis of the Metabolic Profiles of Strains of *Tribolium castaneum* (Herbst) Adults with Different Levels of Phosphine Resistance Based on Direct Immersion Solid-Phase Microextraction and Gas Chromatography-Mass Spectrometry. *Molecules* **2023**, *28*, 7721. [CrossRef]
17. *GB/T16037*; Determination of Phosphine-Ammonium Molybdate Spectrophotometric Method. Chinese National Standard. National Health and Family Planning Commission of PRC: Beijing, China, 1996.
18. Shan, C.; Li, B.; Li, L.; Du, X.; Ren, Y.; McKirdy, S.J.; Liu, T. Comparison of fumigation efficacy of methyl bromide alone and phosphine applied either alone or simultaneously or sequentially against *Bactrocera correcta* in *Selenicereus undatus* (red pitaya) fruit. *Pest Manag. Sci.* **2023**, *79*, 4942–4951. [CrossRef]
19. Kim, K.; Park, M.G.; Lee, Y.H.; Jeon, H.J.; Kwon, T.H.; Kim, C.; Lee, S.E. Synergistic effects and toxic mechanism of phosphine with ethyl formate against citrus mealybug (*Planococcus citri*). *Appl. Sci.* **2021**, *11*, 9877. [CrossRef]
20. Lee, B.H.; Kim, H.M.; Kim, B.S.; Yang, J.O.; Moon, Y.M.; Ren, Y. Evaluation of the synergistic effect between ethyl formate and phospine for control of *Aphis gossypii* (Homoptera: Aphididae). *J. Econ. Entomol.* **2016**, *109*, 143–147. [CrossRef] [PubMed]
21. Alnajim, I.; Agarwal, M.; Liu, T.; Li, B.; Du, X.; Ren, Y. Preliminary Study on the Differences in Hydrocarbons Between Phosphine-Susceptible and-Resistant Strains of *Rhyzopertha dominica* (Fabricius) and *Tribolium castaneum* (Herbst) Using Direct Immersion Solid-Phase Microextraction Coupled with GC-MS. *Molecules* **2020**, *25*, 1565. [CrossRef] [PubMed]
22. Sun, L. Exploration of Factors to Enhance Aromatic Quality in Green Tea. Ph.D. Thesis, Murdoch University, Murdoch, Australia, 2022.
23. Daglish, G.J.; Collins, P.J.; Pavic, H.; Kopittke, R.A. Effects of time and concentration on mortality of phosphine-resistant *Sitophilus oryzae* (L) fumigated with phosphine. *Pest Manag. Sci. Former. Pestic. Sci.* **2002**, *58*, 1015–1021. [CrossRef] [PubMed]
24. Opit, G.P.; Phillips, T.W.; Aikins, M.J.; Hasan, M.M. Phosphine resistance in *Tribolium castaneum* and *Rhyzopertha dominica* from stored wheat in Oklahoma. *J. Econ. Entomol.* **2012**, *105*, 1107–1114. [CrossRef] [PubMed]
25. Pimentel, M.A.G.; Faroni, L.R.D.A.; Tótola, M.R.; Guedes, R.N.C. Phosphine resistance, respiration rate and fitness consequences in stored-product insects. *Pest Manag. Sci. Former. Pestic. Sci.* **2007**, *63*, 876–881. [CrossRef] [PubMed]
26. Jagadeesan, R.; Nayak, M.K.; Pavic, H.; Chandra, K.; Collins, P.J. Susceptibility to sulfuryl fluoride and lack of cross-resistance to phosphine in developmental stages of the red flour beetle, *Tribolium castaneum* (Coleoptera: Tenebrionidae). *Pest Manag. Sci.* **2015**, *71*, 1379–1386. [CrossRef]
27. Tian, X.; Hao, J.; Wu, F.; Hu, H.; Zhou, G.; Liu, X.; Zhang, T. 1-Pentadecene, a volatile biomarker for the detection of *Tribolium castaneum* (Herbst) (Coleoptera: Tenebrionidae) infested brown rice under different temperatures. *J. Stored Prod. Res.* **2022**, *97*, 101981. [CrossRef]
28. Wirtz, R.A.; Taylor, S.L.; Semey, H.G. Concentrations of substituted p-benzoquinones and 1-pentadecene in the flour beetles *tribolium confusum* J. Du Val and *tribolium castaneum* (herbst). *Comp. Biochem. Physiol. Part B Biochem.* **1978**, *61*, 25–28. [CrossRef]
29. Kan, X.; Fan, Y.; Fang, Z.; Cao, L.; Xiong, N.N.; Yang, D.; Li, X. A novel IoT network intrusion detection approach based on adaptive particle swarm optimization convolutional neural network. *Inf. Sci.* **2021**, *568*, 147–162. [CrossRef]
30. Karsoliya, S. Approximating number of hidden layer neurons in multiple hidden layer BPNN architecture. *Int. J. Eng. Trends Technol.* **2012**, *3*, 714–717.
31. Beattie, J.R.; Esmonde-White, F.W. Exploration of principal component analysis: Deriving principal component analysis visually using spectra. *Appl. Spectrosc.* **2021**, *75*, 361–375. [CrossRef]
32. Wang, C.; Feng, Y.; Zhang, S.; Fu, T.; Sheng, Y.; Zhang, Y.; Zhang, D. Effects of storage on brown rice (*Oryza sativa* L.) metabolites, analyzed using gas chromatography and mass spectrometry. *Food Sci. Nutr.* **2020**, *8*, 2882–2894. [CrossRef]
33. Rolo, A.; Teodoro, J.; Palmeira, C. Role of oxidative stress in the pathogenesis of nonalcoholic steatohepatitis. *Free Radic. Biol. Med.* **2012**, *52*, 59–69. [CrossRef]
34. Cocco, T.; Di, M.; Papa, P.; Lorusso, M. Arachidonic acid interaction with the mitochondrial electron transport chain promotes reactive oxygen species generation. *Free Radic. Biol. Med.* **1999**, *27*, 51–59. [CrossRef]
35. Liu, T.; Chen, X.; Sun, J.; Jiang, X.; Wu, Y.; Yang, S.; Du, X. Palmitic acid-induced podocyte apoptosis via the reactive oxygen species-dependent mitochondrial pathway. *Kidney Blood Press. Res.* **2018**, *43*, 206–219. [CrossRef]
36. Wang, N.; Ma, H.; Li, J.; Meng, C.; Zou, J.; Wang, H.; Wang, K. HSF1 functions as a key defender against palmitic acid-induced ferroptosis in cardiomyocytes. *J. Mol. Cell. Cardiol.* **2021**, *150*, 65–76. [CrossRef]
37. Fatima, S.; Hu, X.; Gong, R.; Huang, C.; Chen, M.; Wong, H.; Kwan, H. Palmitic acid is an intracellular signaling molecule involved in disease development. *Cell. Mol. Life Sci.* **2019**, *76*, 2547–2557. [CrossRef] [PubMed]
38. Griffiths, G. Jasmonates: Biosynthesis, perception and signal transduction. *Essays Biochem.* **2020**, *64*, 501–512.
39. Niwa, R.; Niwa, Y.S. Enzymes for ecdysteroid biosynthesis: Their biological functions in insects and beyond. *Biosci. Biotechnol. Biochem.* **2014**, *78*, 1283–1292. [CrossRef]
40. Czuba, E.; Steliga, A.; Lietzau, G.; Kowiański, P. Cholesterol as a modifying agent of the neurovascular unit structure and function under physiological and pathological conditions. *Metab. Brain Dis.* **2017**, *32*, 935–948. [CrossRef]
41. Shen, G.; Zhou, L.; Liu, W.; Cui, Y.; Xie, W.; Chen, H.; Li, H. Di (2-ethylhexyl) phthalate alters the synthesis and β-oxidation of fatty acids and hinders ATP supply in mouse testes via UPLC-Q-Exactive Orbitrap MS-based Metabonomics study. *J. Agric. Food Chem.* **2017**, *65*, 5056–5063. [CrossRef] [PubMed]
42. Bartlett, K.; Eaton, S. Mitochondrial β-oxidation. *Eur. J. Biochem.* **2004**, *271*, 462–469. [CrossRef]

43. Kim, D.; Kim, K.; Lee, Y.H.; Lee, S.E. Transcriptome and Micro-CT analysis unravels the cuticle modification in phosphine-resistant stored grain insect pest, *Tribolium castaneum* (Herbst). *Chem. Biol. Technol. Agric.* **2023**, *10*, 88. [CrossRef]
44. Shen, X.; Che, M.; Xu, H.; Zhuang, X.; Chen, E.; Tang, P.; Wang, K. Insight into the molecular mechanism of phosphine toxicity provided by functional analysis of *cytochrome b5 fatty acid desaturase* and *dihydrolipoamide dehydrogenase* in the red flour beetle, *Tribolium castaneum*. *Pestic. Biochem. Physiol.* **2023**, *194*, 105482. [CrossRef]
45. Zuryn, S.; Kuang, J.; Ebert, P. Mitochondrial modulation of phosphine toxicity and resistance in *Caenorhabditis elegans*. *Toxicol. Sci.* **2008**, *102*, 179–186. [CrossRef] [PubMed]
46. Kim, H.K.; Lee, S.W.; Kim, J.I.; Yang, J.O.; Koo, H.N.; Kim, G.H. Synergistic effects of oxygen on phosphine and ethyl formate for the control of *Phthorimaea operculella* (Lepidoptera: Gelechiidae). *J. Econ. Entomol.* **2015**, *108*, 2572–2580. [CrossRef] [PubMed]